Fatigue life improvement using low transformation temperature weld material with measurement of residual stress

Jordan Franks, Greg Wheatley, Pedram Zamani, Reza Masoudi Nejad, Wojciech Macek, Ricardo Branco, Farzaneh Samadi

PII: S0142-1123(22)00393-0
DOI: https://doi.org/10.1016/j.ijfatigue.2022.107137
Reference: JIJF 107137

To appear in: *International Journal of Fatigue*

Received Date: 30 April 2022
Revised Date: 6 July 2022
Accepted Date: 11 July 2022

Please cite this article as: Franks, J., Wheatley, G., Zamani, P., Masoudi Nejad, R., Macek, W., Branco, R., Samadi, F., Fatigue life improvement using low transformation temperature weld material with measurement of residual stress, *International Journal of Fatigue* (2022), doi: https://doi.org/10.1016/j.ijfatigue.2022.107137

Fatigue life improvement using low transformation temperature weld material with measurement of residual stress

Jordan Franks[1], Greg Wheatley[1,*], Pedram Zamani[2], Reza Masoudi Nejad[3], Wojciech Macek[4], Ricardo Branco[5], Farzaneh Samadi[6,*]

[1]College of Science and Engineering, James Cook University, Townsville QLD 4811, Australia

[2]Department of Mechanical Engineering, Faculty of Engineering, Ferdowsi University of Mashhad, Mashhad, Iran

[3]School of Mechanical and Electrical Engineering, University of Electronic Science and Technology of China, Chengdu, 611731, China

[4]Gdansk University of Technology, Faculty of Mechanical Engineering and Ship Technology, 11/12 Gabriela Narutowicza, Gdańsk 80-233, Poland

[5]University of Coimbra, CEMMPRE, Department of Mechanical Engineering, Coimbra, Portugal

[6]Department of Materials, Faculty of Engineering, Semnan University, Semnan, Iran

Abstract

Welding processes often produce high levels of tensile residual stress. Low transformation temperature (LTT) welding wires utilise phase transformation strains to overcome the thermal contraction of a cooling weld. In this paper, the residual stress within each weld was quantified using the milling/strain gauge method, being the strain change measured as the weldment was milled away. The fatigue tests were conducted under uniaxial loading considering two types of LTT materials. The results show that the crack propagation of all samples was similar in cycles although both LTT materials extended the crack initiation, and, therefore, the overall life of the part. It was found that both LTT materials reduced the residual tensile stresses, increased the residual compressive stresses, leading to increase in fatigue life about 30%.

Keywords: Residual stress; Fatigue life; Heat affected zone; Low transformation temperature; Scanning electron microscope.

1. Introduction

Residual stress is a major factor in the lifespan of a welded structure [1-7]. In essence, residual stress is known as an internal force without the addition of any external forces [8, 9]. All weld fillers are prone to residual stress due to the phase changes during the cooling process. Traditional weld techniques and weld fillers are susceptible to high concentrations of residual stress because of the phase change from austenite to martensite, i.e. the transformation from a liquid to a solid [10-12]. Measuring the residual

* Corresponding authors.

E-mail addresses: jordan.franks@my.jcu.edu.au (J. Franks), greg.wheatley@jcu.edu.au (G. Wheatley), p.zamani@alumni.um.ac.ir (P. Zamani), masoudinejad@uestc.edu.cn (R. Masoudi Nejad), wojciech.macek@pg.edu.pl (W. Macek), ricardo.branco@dem.uc.pt (R. Branco), frzn.samadi@gmail.com (F. Samadi).

stress through a weld is crucial to understanding the extent of the residual forces. There are many ways to measure the residual stress through a structure, the procedure falls under one of three categories: destructive, semi-destructive or non-destructive [13-15]. Non-destructive techniques use X-ray, neutron diffraction, ultrasonic and magnetic methods. Destructive techniques allow for the calculation of initial residual stress through removing material from the specimen while measuring the strain along the opposing edge. The residual stress in the weld applies a force to the plate, as the material is removed the strain will increase, from this, the initial residual stress can be calculated [16-18].

Fatigue is among the most common reasons for structural failure; fatigue failure involves 3 stages, crack initiation, crack propagation, and total failure. After a series of cyclic loading, a crack initiates, which then propagates through continual use, leadings to a catastrophic failure [19, 20]. Asgarian et al. [21] evaluated the fatigue life of steel connections in a jacket platform using S-N curves proposed in API RP2A. The results show that the formulas in the new edition of standards consider more fatigue strength than previous ones. Zhang et al. [22] investigated the effects of fire-induced high temperatures on the residual punching shear strength of reinforced concrete flat-plate structures after cooling and to examine the effectiveness of a detailing approach for enhancing the post-punching load-carrying capacity. A structures life depends on the quality of each component along with the process of production and maintenance throughout its life. During manufacturing, treatments can be performed to increase the fatigue life, such as shot peening or stress relief, as this reduces the residual stress in the weld. Stress rising factors can decrease the life of a component by increasing the stresses through a critical point, this is often the toe of a weld [23]. By reducing the transformation temperature from austenite to martensite, the weld filler can retain its austenite properties. Standard weld fillers have an Ms temperature of approximately 450℃, whereas the most common LTT fillers exhibit a Ms temperature in the range from 200 ^{0}C to 400 ^{0}C [24-26]. If the Ms temperature is far above 200 ^{0}C, it is proven that once the transformation is complete, the weld continues to shrink, causing excessive residual tensile stresses. In contrast, if the filler Ms temperature is far below 200 ^{0}C, the transformation from austenite to martensite is then incomplete as it begins too close to ambient. With an ideal LTT material, the transformation begins at approximately 200 ^{0}C and the weld continues to expand until it reaches ambient. This introduces residual compressive stress, which improves the mechanical properties [27, 28]. The temperature of the Ms transformation is dependent on the chemical properties of the filler. Austenite stabilising elements have a significant impact on the outcome of a weld. Nickel (Ni), chromium (Cr), and carbon (C) are all key elements in the outcome of an LTT weld filler. Nickel controls the transformation temperature, chromium allows for the retention of austenite properties, and carbon content controls the hardness of the cooled weld [29-31].

In the phenomenon of HCF failure, which occurs due to repetitive stress and begins with the occurrence of microcracks and grows under the influence of cyclic stresses, the amount of maximum stress is usually less than the yield strength of the material [32-34]. One of the most important challenges in

fatigue analysis is to determine the life of components because damage in HCF occurs at stresses less than yield stresses and at the microscopic scale in defects of the material and even when the damage is growing, there is no sign of failure [35-37]. Cracks are considered a major defect in welded structures; cracks develop through a structure due to stress, and can lead to catastrophic failure [38]. Cracks can be classified as either hot, cold, or residual cracks [39, 40]. Hot and cold cracks develop during the application and cooling of a weld. Fatigue cracks occur over time, their development and progression are dependent on the material, environment and applied loading. Conventional welding wire generally provides a fatigue strength below that of the base material, the high tensile residual stress within a weld filler greatly reduces its overall tensile strength [18]. It has been proven that the use of an LTT weld filler reduces the residual stress and greatly increases the life of the welded part [25]. Wheatley and Ohta stated that crack propagation in both LTT and regular weld fillers is very similar, although the crack initiation time for LTT fillers is prolonged and therefore extends the overall life of the component [41].

Hot cracking is a defect within welds that occurs during the cooling process. Cracks can develop as the weld filler shrinks during the cooling process. While cooling, hot cracking occurs in the solidification phase where the weld filler shrinks, producing microscopic gaps in the weld material, especially at the weld toe [42]. Karlsson et al. [43] compared a number of alloying elements and found that hot cracking is more prominent in LTT materials using nickel as its primary alloying element. This is caused by the solidification process occurring as austenite. Hot cracking has not had a large focus in previous literature due to its small contribution to the overall outcome of a weld, cold cracking plays a larger role in welded structures. Cold cracks occur in the heat-affected zone (HAZ) and through the cross-sectional area of a weld, although LTT materials have shown a significant decrease in cold cracking, there is still the need for further research into cold cracking and the prevention for certain fillers [43]. Cold cracking occurs when hydrogen pockets develop within a weld, this can be caused by the filler material, improper preparation or due to an excessive phase transformation [44]. As LTT materials reduce the internal residual stress, they therefore reduce the risk of cold cracking, simply by reducing the production of pockets in the weld. Fillers with higher C content tend to be more susceptible to cold cracking due to the hard, brittle structure. Studies have shown that the use of LTT can negatively affect the fracture toughness [24]. This is caused by the increase in carbon content within the weld, the hard/brittle structure that comes with a higher carbon content. LTT materials displaying a low fracture toughness are not common in industry as they require post weld treatments to gain a satisfactory standard [45]. To accommodate for this, LTT weld fillers in use have a low carbon content, typically C<0.6wt% [46].

LTT materials have significantly changed the process of high-quality welds. Their capabilities have rapidly reduced the need for post-processing operations, such as heat treating or shot peening, which is a very positive aspect for modern industry. In addition, the reduction in residual stress can dramatically increases the fatigue life of a structure. Nevertheless, due to the variety of elements within LTT fillers,

which can result in different properties, extensive research is required to fully understand the effect of each elemental composition on the mechanical response, particularly under cyclic loading. In both ferrous and non-ferrous metals, there is a need for an increase in hot and cold cracking prevention, ductility control and multi-pass applications. The depth of research into this field is very extensive although much more is required for definitive results. This paper aims at addressing the effect of the LTT filler on residual stress fields and fatigue lifetime.

2. Materials and Methods

The chemical composition and the mechanical properties of the materials used in the experimental tests were obtained following the methodology proposed by Wheatly [41]. The chemical composition is summarised in Table 1 while the mechanical properties are listed in Table 2. The tested materials consisted of two mild steel LTT weld fillers and three industry fillers (1 mild steel and 2 stainless steel). The base material was a hardened mild steel, selected due to its consistency in terms of industry application and relevance for engineering. The experimental tests comprised two different analyses. First, destructive tests were conducted using a milling machine and strain gauges to quantify the changing residual stress through the milling application. Then, fatigue tests were conducted at a high load and a high-frequency until failure. Figure 1 shows the proposed geometry used in the tests. The construction is the most important part of these coupons because, the addition of heat changes both the molecular microstructure and the chemical composition of the steel. The specimens were manufactured by welding a 200 mm section, as schematised in Figure 1, and then cold and cut into 50 mm strips. This was done to reveal the welded section in order to analyse the HAZ region.

Table 1. Chemical composition of the materials used in the experimental tests (in wt%) [46].

Material	Cr	Ni	C	Mn	Si	S	K	Mo	P	Cu
LTTA (BOHLOR-Ti-60T)	-	0.85	0.07	1.3	0.45	-	-	-	-	-
LTTB (LINCOLN-71E- H)	-	-	0.04	1.4	0.6	0.01	0.013	-	-	-
Industry filler (Cigweld -LW1)	-	-	0.08	1.16	0.7	0.01	0.015	-	-	-
Base Material (HARDOX 500)	1.5	1.5	0.3	1.6	0.7	0.01	0.02	0.6	-	-
Sample 4 (Tetra S 307-G)	19	9	0.1	6	0.7	0.08	-	-	0.02	-
Sample 5 (BOC 307Si)	17	7	0.7	6.8	0.01	0.01	0.013	0.1	0.02	0.12

Table 2. Mechanical properties of the materials used in the experimental tests [46].

Material	LTTA (BOHLOR-Ti-60T)	LTTB (LINCOLN-71E- H)	Industry filler (Cigweld - LW1)	Base Material (HARDOX 500)	Sample 4 (Tetra S 307-G)	Sample 5 (BOC 307Si)
Yield Strength (MPa)	550	570	450	1400	480	450
Tensile Strength (MPa)	610	620	550	1580	630	650
Elongation (%)	25	25	9	7	40	40

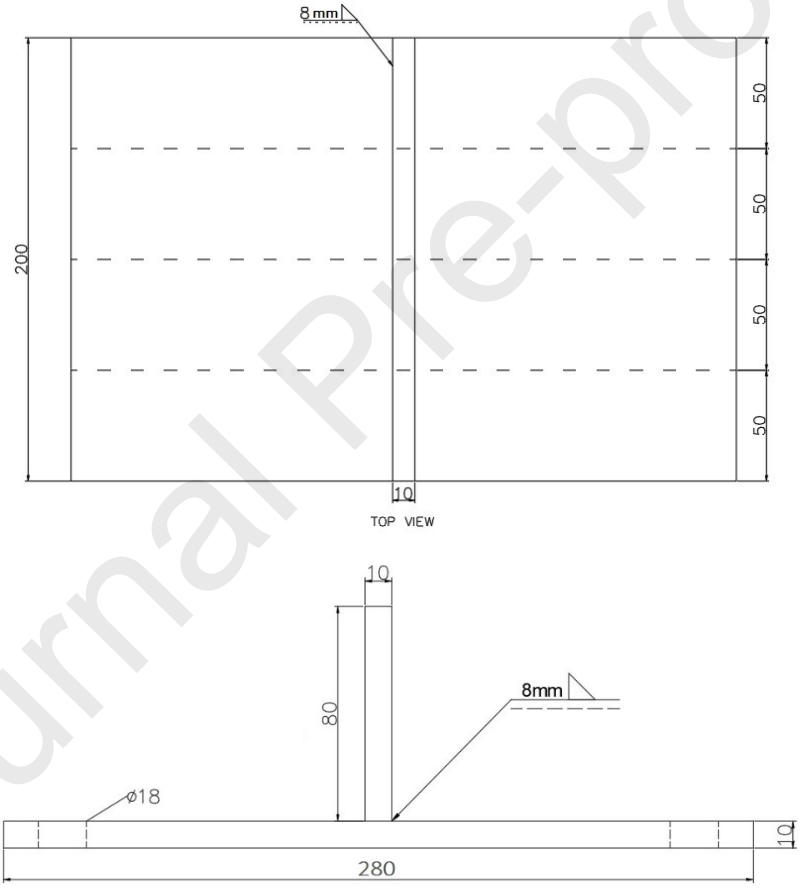

Figure 1. Geometry of the specimens used in the experimental tests (dimensions in mm).

Hardness testing was done on each sample as an assessment of the effects of welding. The hardness of each weld section, the HAZ and the unaffected steel was conducted. This testing was aimed to show the alterations to the metal through the applied heat. Figure 2 shows the points for hardness measurement and scanning electron microscope examination.

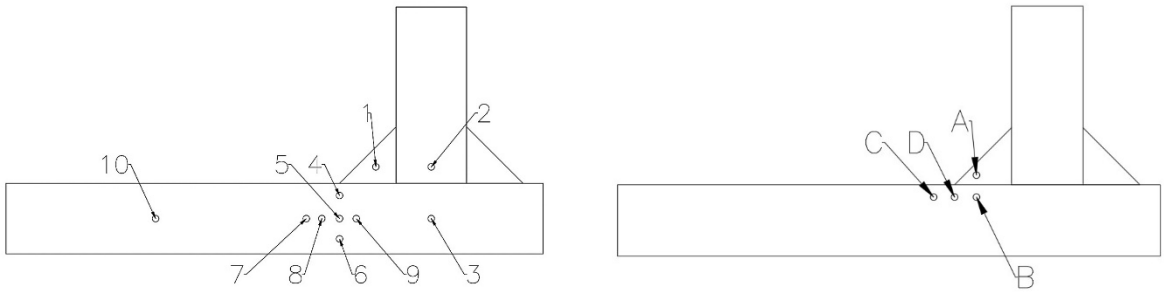

(a) (b)

Figure 2. The points for: (a) hardness testing; (b) scanning electron microscope examination.

Rockwell HRB was chosen for the hardness testing, as it has a broad scale surrounding the hardness of Hardox 500. Points 1, 2, 3 and 10 showed the maximum difference between each zone whereas points 4-9 were aimed to identify the hardness gradient across the HAZ. The scanning electron microscope was used to analyse the weld section and the parent metal. A small section of the welded area was cut and placed in the microscope, to show the different microstructures surrounding the weld, identifying changes occurred during the addition of heat and external elements. Figure 2-(b) shows the section used in the microscope with each critical point analysed for chemical composition. The residual stress was quantified using the destructive milling method. One sample of each specified weld filler was analysed. The T specimen was wiped clean with isopropyl alcohol to ensure a clean surface for the strain gauges. Two strain gauges were attached to the opposing side to the weldment as shown in Figure 3 (Bestech FLAB-5-11-3LJC-F strain gauges secured with Eythl 2-Cyanoacrylate). The weld and tongue were milled away in increments of 0.5 mm. The strain and overall thickness were recorded after each pass of the computer numerical control (CNC) router. Once the weldment had been entirely milled away, stress measurements were processed with the specified equations for the calculation of the initial residual stress.

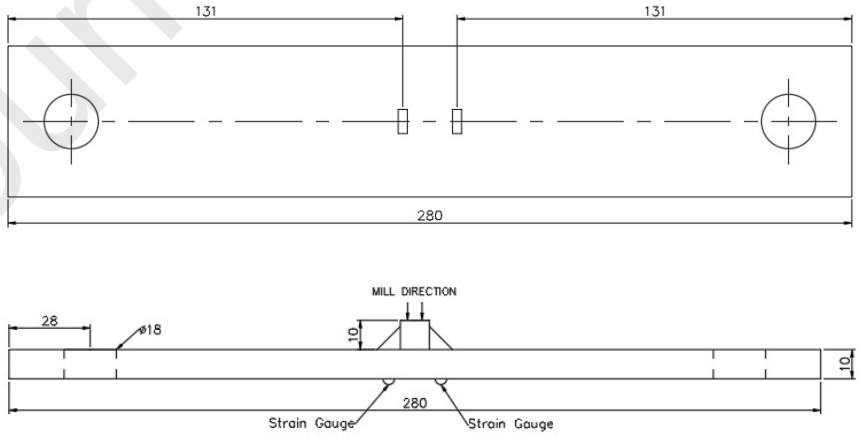

Figure 3. Installation of the two strain gauges on the sample (dimensions in mm).

Fatigue testing was conducted using an Instron 8800 servohydraulic machine. A metallic frame was constructed allowing the test specimen to be held firmly throughout the fatigue cycling. The

experimental test setup shown in Figure 4. The frame is firmly mounted into the testing machine with the specimen bolted on top, then connected to the hydraulic ram. The fatigue tests were conducted under pulsating loading conditions with a cycle frequency of 5 Hz and a maximum load of 24 kN. Several safety elements were programmed to eliminate the likelihood of the parts projecting off, such as the maximum allowable force and the maximum displacement, with an automatic shutdown. Using the testing machine with a precise programmed loading pattern, it was eliminated any human error from the fatigue testing phase. Each specimen was run until complete failure, with a maximum displacement of 10 mm. Details about the load pattern as well as about the normal force and the bending moment diagrams, are exhibited in Figure 5.

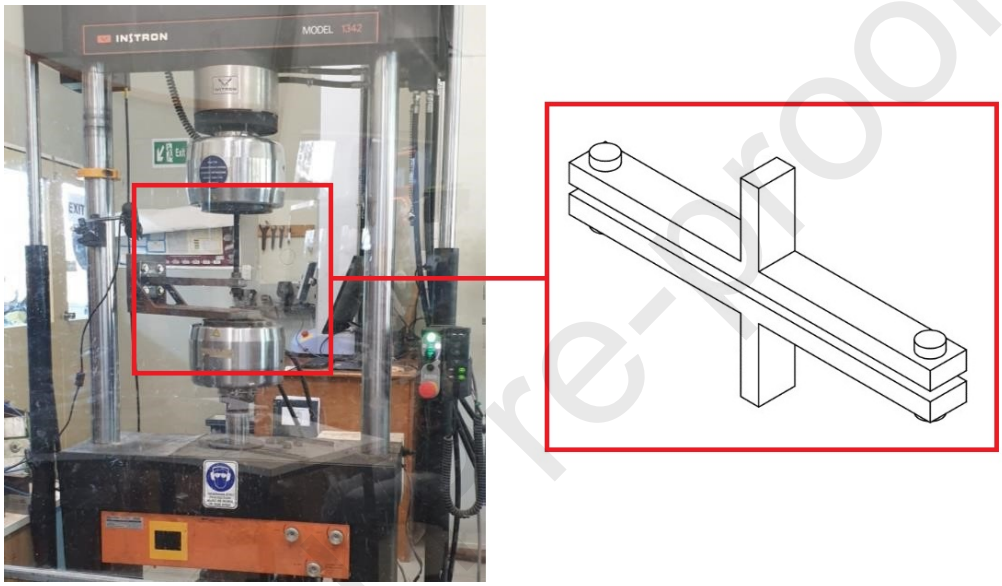

Figure 4. Experimental test setup.

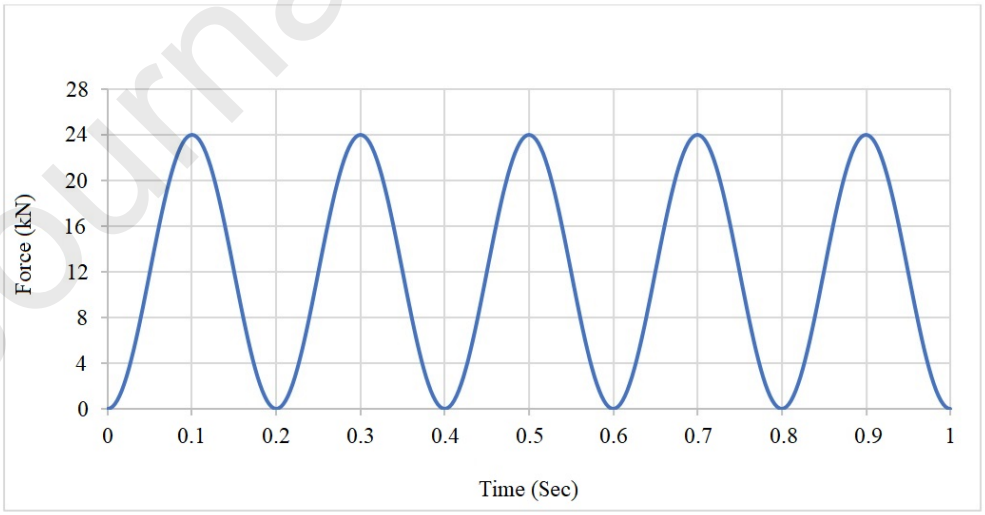

(a)

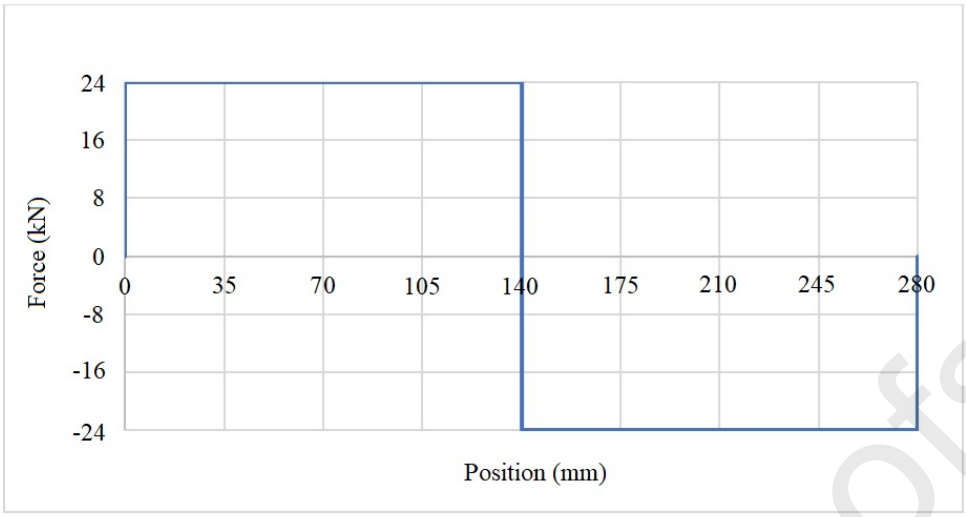

(b)

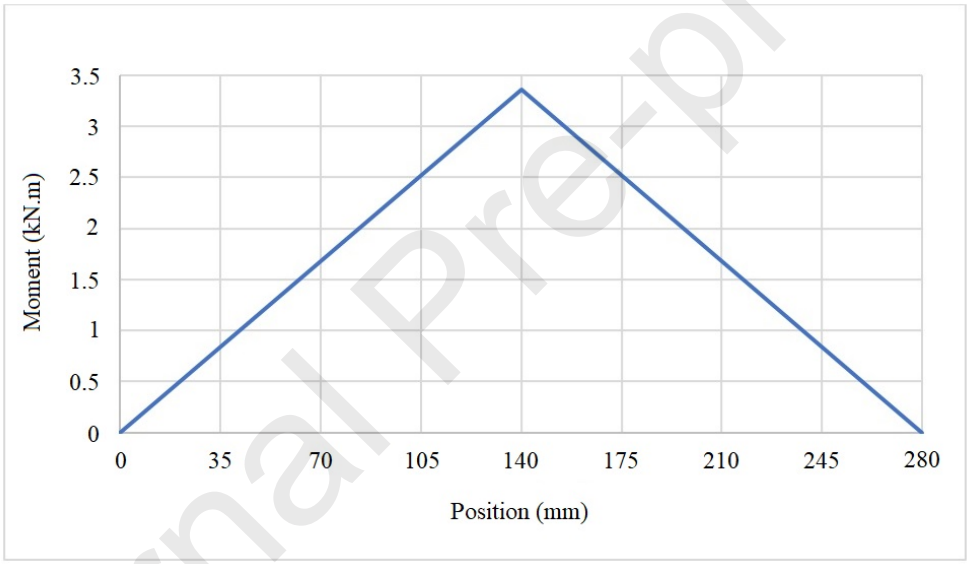

(c)

Figure 5. The testing apparatus: (a) load pattern; (b) normal force diagram; and (c) bending moment diagram.

3. Results and discussion

3.1. Computational Fatigue Analysis

The numerical model was designed in ANSYS finite-element software. Fatigue loading was applied similarly to that applied in the experimental tests. The computational fatigue analysis was done as a comparison to the real-life testing. Figure 6 shows the generated mesh along with the maximum and minimum life points. Table 3 shows the computed results for different numbers of mesh elements. This allows the observation of the mesh convergence and the computation accuracy of the analysis. The

results from the FE analysis showed convergence, with a difference less than 1%, which was deemed acceptable.

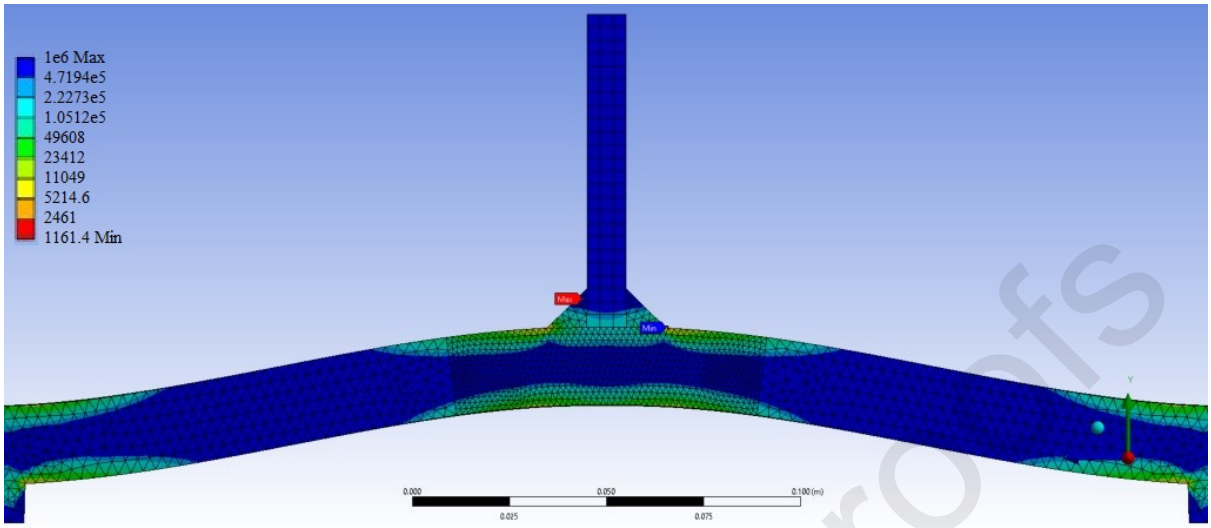

Figure 6. Computational model for the generated mesh along with the maximum and minimum life points.

Table 3. Finite element results for different number of elements.

Nodes	Elements	Minimum Cycles	Percentage Change
18836	5472	1747.4	NA
40354	19473	1153	-34.02%
74700	43397	1291.6	10.74%
156905	102210	1165	-9.81%
212966	144101	1163	-0.18%
250126	169900	1161.4	-0.14%

The results from the computational analysis did not give any major conclusions, except the fact that compared to the actual tests, it gave a much lower fatigue life: 1161 cycles rather than approximately 4500 cycles for the actual tests. The finite element analysis showed that the point with the highest stress and shortest life was the point where the weld met the base plate (i.e. the weld toe). This was consistent with the physical tests, since the cracks always initiated in the samples on this point. The heat effects on the welds and parent metal are extremely difficult to simulate and would require large amount of research to compute accurately, as this is a reasonably new study and therefore has limited past literature. Although the weld effects are scarcely considered, the approximate fatigue life was still computed. The fatigue analysis performed gave a very short life when compared to the actual testing. This may be due to several unknown factors, such as low allowable elongation, inconsistent join factors, or differing weld properties, just to mention a few. Although minor factors can make phenomenal differences in a computational analysis, it was expected that the analysis would outline the actual results

due to no heat effects on the steel. It is possible, however, to include a maximum stress riser surrounding weld processes in the FE analysis of ANSYS and, as a result, the theoretical life of the part is reduced. The computational analysis was done as a reference for practical testing. The fatigue analysis showed that the designed specimen would only last 1161 cycles for the applied loading pattern. Although mesh convergence was performed to assure an accurate analysis, the study did not show significant likeness to the actual testing. The main conclusions from this numerical simulation were the points of failure and the observations of stress flow. It is recommended that future research develop more accurate simulations to analyse fatigue patterns, crack growth and material changes.

3.2. Experimental test adaptations

Through pre-testing there were several difficulties and challenges to overcome. The manufacturing of the specimens was a major part in the accuracy and effectiveness of the testing. Initially the specimen's base metal was to be 20 mm thick but due to materials availability it was constructed with 10mm. The length was also meant to be 400 mm, but due to size constraints on the JCU cold saw, they were trimmed to 280 mm. The initial test specimens had to be shortened to fit in the band saw correctly. Due to this the M18 holes were closer to the middle, about 4 cm from the centre. This highly restricted the flex applied to the weld and the applied force was acting more as a shear force, simply ripping the weld apart, rather than applying a fatigue cycle. The holes were then re-drilled 28 mm from either end, this position allowed significant flex across the coupon, with a high amount of tension applied to the weld. This method resulted in a clean break along the toe of the weld. This method gave reasonably consistent results, although the thinner base allowed the HAZ zone to play a major role in the life of the sample. The holes for the majority of the samples had to be cut out using the water jet cutter, this was a much quicker and easier method. As a result of the difficult manufacturing many of the samples ranged in width from 52 mm down to 48 mm. The difference between each sample gave several discrepancies for fatigue life, as the applied stresses were lower across a larger cross section. Due to several discrepancies in the results, extra samples from each wire were tested for fatigue life, and two new welding wires were tested allowing for a broader study, 'Tetra S 307-G' and 'BOC 307Si' are represented by samples 4 and 5 respectively.

3.3. Residual Stress

Figure 7 shows residual stress field against position from top of plate for mild steel fillers, LTTB and stainless fillers. The calculated residual stress is also presented in Table 4. Overall, both LTT weld fillers showed reduced residual stresses when compared to all other weld wires. The Cigweld wire began in compression for the initial 4 mm, it then transferred to residual tensile forces, with a maximum occurring at approximately 3 mm. LTTA had mainly residual compressive stress with only slight tensile stresses applied. LTTA experienced mostly compressive forces until the weld was almost completely

milled away. LTTB was similar to LTTB with he applied stresses until the weld was completely milled away. The BOC weld filler had the highest tensile forces. Initially it had compressive forces lasting until a position of 5mm where the tensile forces began increasing as the weld was milled away. The BOC weld filler experienced tensile forces almost 10 times more than the LTT weld fillers. The Tetra weld filler experienced phenomenal amounts of compressive stresses, consistent compressive stress until approximately 1 mm from the base.

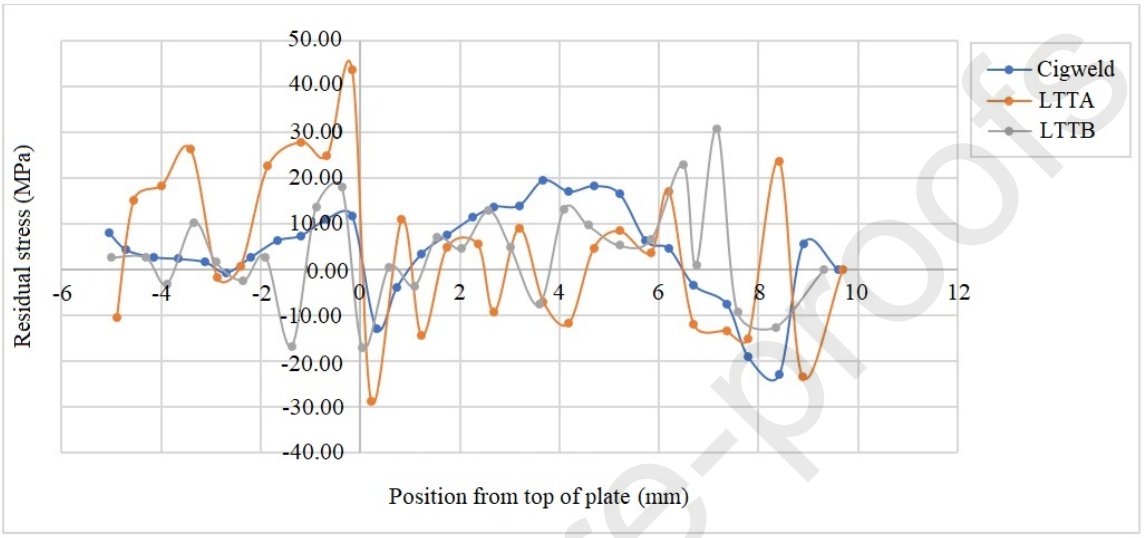

(a)

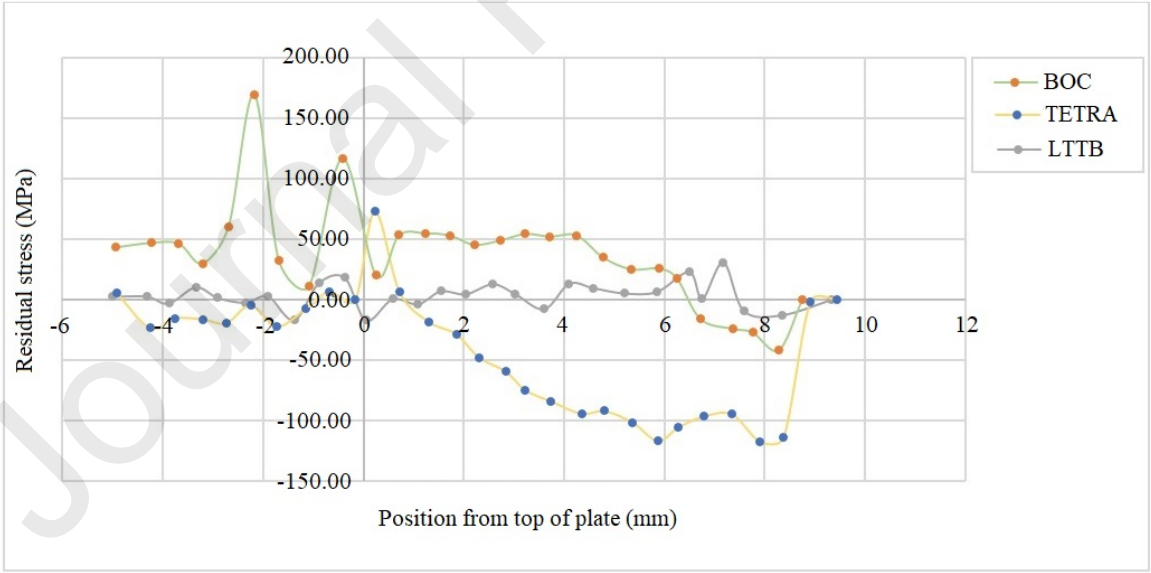

(b)

Figure 7. Residual stress field against position from top of plate for: (a) Mild steel fillers; and (b) LTTB and stainless fillers.

Table 4. Calculated Residual Stress

Type	Tensile (MPa)	Compression (MPa)	Total (MPa)
Cigweld	-70.31	196.43	126.12
LTTA	-147.42	267.96	120.54
LTTB	-72.29	171.11	98.82
TETRA	-1355.77	92.35	-1263.42
BOC	-108.55	1096.38	987.82

There are many factors that may affect the accuracy of the results in this testing method. The first 2 milling passes on LTTA were done with the strain gauge wires crossed, this was identified by the varying readings in the graphs. After the wires were straightened the gauges were not zeroed but instead for the calculations this was marked as the zero value for the strain readings. A significant defect was present in LTTA. This hot crack was the only one identified with a significant enough size to be worth noting. The milling machine was able to cut 0.5 mm quite accurately, although as the residual tensile stress was released, the samples flexed, altering the cut depth. For consistency, the thickness after each cut was recorded. Each thickness measurement was done with digital vernier callipers in order to reduce human error. The restraining method was highly likely to apply an external force to the specimens as the bolts were extremely tight. This restraining method was a contributing factor to the readings experienced in the milling of the base plate.

Both LTT materials displayed the exact phenomena expected. They showed increased compressive forces rather than tensile. LTTA had a residual stress measurement of 120 MPa while LTTB had 98 MPa, when compared to the industry weld filler with 126 MPa. All three mild steel weld fillers had an overall compressive/tensile stress significantly less than both stainless wires. Both the LTTA and LTTB fillers had compressive stresses within the weld which is likely due to the austenite stabilisers. The different chemical compositions allowed for the retention of austenite and the reduction of tensile forces. LTTB experienced tensile stresses within the last 2 mm of the weldment. This was possibly caused by an altered chemical composition, through mixing with the parent material. The industry fillers exhibited initial compressive forces which were likely caused by the initial rapid cooling. The rapid cooling increased the martensite transformation strains which overcame the thermal contraction strains. Previous literature shows that the industry filler displayed a typical stress distribution, with an initial compressive stress and a final tensile stress. The BOC stainless wire showed a similar pattern to the industry standard Cigweld filler. Nevertheless, it experienced significantly more tensile stresses. The increased tensile stress was likely caused by the significantly reduced silicone content. The Tetra welding wire had excessive levels of residual compressive stress. The complete compressive stresses are likely due to the increased amount of chromium, nickel, and silicone, as each of these elements are used to retain austenite in metals.

Hot cracking was not noticed in most specimens, the only substantial crack was in LTTA. The defect in LTTA is most likely caused by the addition of nickel. This is consistent with literature as Karlsson et al. [43] identified a similar phenomenon relating nickel content and hot cracking. All welding wires experienced small amounts of tensile and compressive forces within the initial layers of the base plate. The overall residual stress did not change much through the layers of the base plate. The measured residual stress in the base plate was likely caused by the addition of forces in the HAZ and the external forces applied during the installation of the specimen into the milling machine. Each specimen was bolted into the CNC, extremely tight to reduce vibrations which was highly likely to cause external forces, leading to discrepancies in the final measurements. Due to the limited space inside the milling machine, special care was taken during the measurement of the depth after each cut. At least, two measurements at different locations were done.

3.4. Fatigue Life

Initially each test was run for 2000 cycles with a video camera, recording the phases of failure. The first 2 rounds of testing were performed on the testing machine. Then, the recorded data was analysed for crack initiation which showed that the testing machine was only retaining the final 10 cycles, meaning the data could not be analysed for the exact crack initiation. The crack initiation was only approximately known through observations. After the first 2 rounds of testing failing to supply accurate crack initiation, it was decided that another 2 rounds would be performed for a more accurate average. A Small video camera was installed to observe the stages of failure. The testing machine was then set to record 1000 cycles and the number of cycles in each test was reduced to 500. This allowed a periodic analysis of the welded structure, enabling a more accurate observation of the developed defects. The recorded data was graphed in excel and the exact crack cycle was determined by an irregular increase in flex, as shown in Figure 8. The crack initiation point was found by observing a sudden change in position (flex) gradient. The specimen in the testing machine suffered a linear increase in flex until the part cracked and, then, the flex gradient suddenly increased. The point was observed closly with a graph displaying approximately 10 seconds either side to distinctly show the cycle number. The results from the fatigue testing can be seen in Table 5, which shows the averaged cycles from each material.

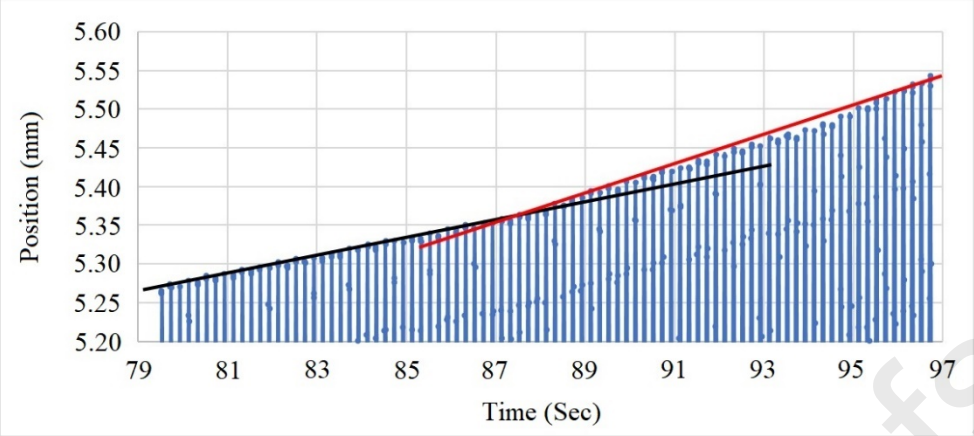

Figure 8. Position against time.

Table 5. Fatigue life results for different materials.

Type	Crack Initiation	Structural Failure
Industry Standard (Cigweld LW1)	2841.5	2972
LTTA (Bohler T160T)	4015	4429
LTTB (Lincoln 71E-H)	2719	3777
Stainless A (TETRA 3 307-G)	3782	4833
Stainless B (BOC 307Si)	2687.5	4890.5

The fatigue life testing showed promising results for the LTT materials. Both LTT wires outperformed the industry standard by approximately 30% fatigue life. The crack initiation for the industry standard wire was approximately 95% of its life, whereas the LTTA and LTTB crack initiation lives were 90% and 81% respectively. The two stainless weld fillers gave very good fatigue life results, approximately 40% longer than the industry wire, and 20% better than both LTT wires. This was expected because high levels of chromium drastically increase fatigue properties, as chromium is a widely used additive in LTT fillers. The fatigue life results showed that both LTT fillers had an increased fatigue life. The Lincoln welding wire had a fatigue life 21% longer then the Cigweld, whereas the Bohler had an increase of 32% fatigue life. The increase in fatigue life was expected due to the proposed properties of each welding wire. There are a number of possible reasons for the increased fatigue life across the specimens. The fatigue life increase is largely due to the decrease in residual stress, and LTTB was found to have the lowest residual stress when compared to the LTTA and the industry weld filler. It is possible that the increase in fatigue life is partially due to the higher tensile strength, although this is unlikely as the tensile strength is only 10% higher in the LTT fillers. The increase in fatigue life from the mild steel weld fillers to the stainless-steel was quite significant. This is possibly due to the high

chromium and nickel contents, which increased the mechanical properties. Both weld fillers had a significantly increased elongation percentage, which likely allowed a more even distribution of stress through the weld.

Nevertheless, the increased fatigue life is clearly not a result of reduced residual stress as both BOC and TETRA had significant amounts of compressive and tensile stresses. There is limited literature surrounding the implication of mild steel LTT weld fillers. This is likely due to the prominence of chromium in industry today. Focussing on the mild steel wires, the chemical compositions only varied slightly. Overall both LTT materials had a smaller carbon content. The lower carbon is likely to allow a more ductile microstructure. LTTA outperformed LTTB, it also had the addition of nickel, nickel is a key element for reducing a materials transformation temperature. The manganese in both LTT materials is significantly more than in the industry filler, as manganese aids in grain refinement which can increase the mechanical properties [47].

3.5. Weld Analysis

A weld section analysis was conducted to determine any changes through the welding procedure. A series of hardness tests, along with a SEM analysis was done for additional information leading to an in-depth explanation of the effects to the parent material after welding. One sample from each material was chosen for hardness testing, Rockwell HRB method was used as the designated testing method. The hardness testing results are presented in Table 6.

Table 6. Hardness testing results.

No.	Industry Filler	LTTB	LTTA
1	82.2	89.7	90.3
2	101.7	89.4	88.4
3	100.25	110.9	106
4	102.2	97.5	89.4
5	101.4	96	92.2
6	106.2	105.4	105
7	116.7	102.8	108.4
8	112.2	85.4	97.8
9	101.3	97.67	96.8
10	115.6	111.5	114.8

The hardness testing showed positive results, in all 3 weld sections the hardness was lower than the parent metal. Point 2 showed that the standard weld filler left the parent metal harder than both LTT fillers. Point 3 showed that the standard filler left a slightly softer structure than either of the LTT fillers.

Points 4-6 showed an interesting pattern, all materials had a softer matrix for points 4 and 5. Point 6 was significantly harder, more so for the LTT fillers than the industry filler. The LTT fillers did not change much between points 4 and 5 but got significantly harder from 5 to 6. When analysing the points from left to right (i.e. 10, 7, 8, 5, 9 and 3, respectively), both LTT materials display a similar pattern, where the hardness reduces reaching its minimum at 8 and 5, then increases at points 9 and 3, as shown in Figure 9. In general, points 4, 5, 8 and 9 were softer than the surrounding metal, this is to be expected as these points are the most likely to correlate to the HAZ. Table 7 displays the data as a difference in wt% compared to the base material. This allows for a definitive difference for each point.

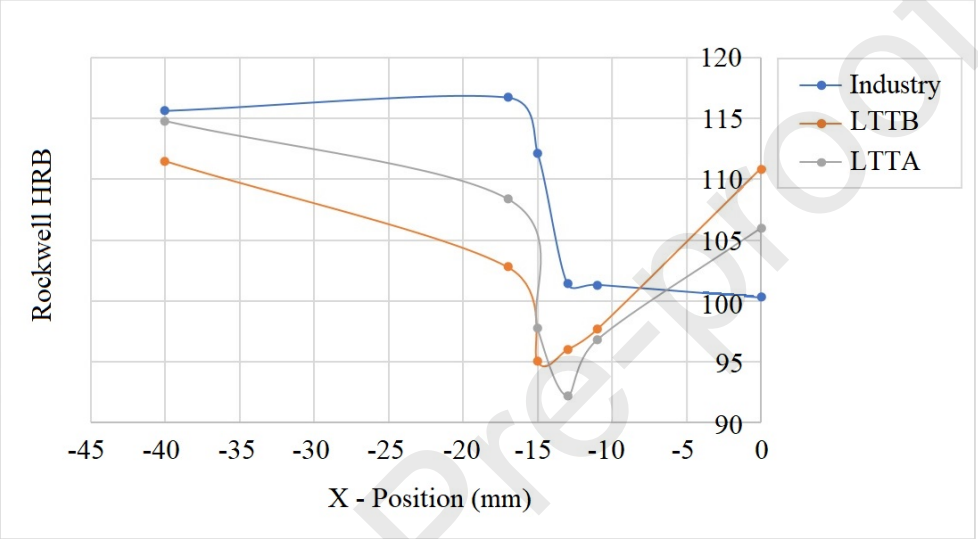

Figure 9. Hardness profile for different materials.

Table 7. Chemical composition for different points.

Element	Point A			Point B			Point C			Point D		
	CIGW ELD	LT TA	LT TB	CIGW ELD	LT TA	LT TB	CIGW ELD	LT TA	LT TB	CIGW ELD	LT TA	LT TB
Mg	-0.05	0.01	-0.06	-0.08	0.08	-0.10	-0.03	0.06	0.21	0.09	0.17	0.17
Al	-0.11	0.05	-0.05	0.32	0.08	0.19	-0.15	0.12	-0.05	0.11	0.15	0.19
Si	0.09	-0.14	8.10	-0.24	0.06	1.61	-0.40	-0.25	-0.29	0.34	-0.09	-0.34
Cl	0.07	-0.03	-0.03	-0.04	0.01	0.00	0.08	-0.03	-0.03	0.05	0.04	0.02
K	0.03	-0.04	-0.03	0.01	0.01	0.00	0.00	0.03	-0.03	-0.02	-0.03	-0.02
Mn	0.48	0.46	0.33	0.03	0.65	0.40	-0.07	-0.08	-0.07	0.40	-0.04	-0.07
Fe	-0.45	-0.47	-8.30	-0.09	-0.69	-2.27	0.76	0.12	0.75	-0.71	-0.20	0.03

The results from the scanning electron microscope (SEM) examination did not show any major differences between the unaffected metal, the weld section and the heat affected zone. This is surprising, as trace amounts of different elements can have a significant difference on the mechanical properties of a material. The study is lacking three major elements: carbon, molybdenum, and chromium, each of which has a major impact on the properties of steel. Although the SEM results did not include the three elements mentioned above, the results are still consistent for other important elements such as,

manganese, silicone, and aluminium. Point A was positioned on the weld, this was important to analyse the difference between the untouched base metal and the pure weld. Looking at the trends for point A, it shows that the manganese percentage was higher in all welds. Figure 10 shows the definitive increase in manganese percentage. This figure displays the manganese measurements as a scanned image, where the weld is shown by the lighter orange containing points A and B, whereas the parent metal is shown by the darker orange containing points D and C.

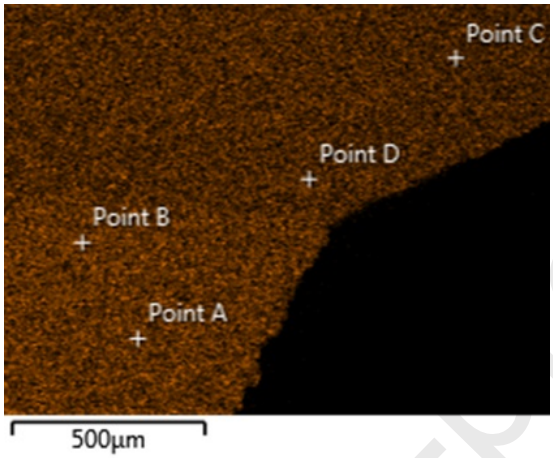

(a)

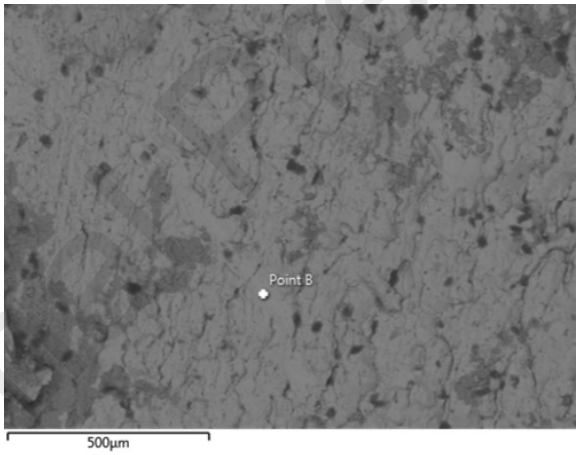

(b)

Figure 10. The definitive increase in manganese percentage: (a) manganese scan sample LTTB; and (b) scanning electron microscopy image.

Point B showed a number of trends for all three weld materials. The manganese was consistently higher than in the base metal, although both LTTA and LTTB were significantly higher. The silicone content at point B shows that LTTB has a significantly higher percentage (approximately 1.5%). This is consistent with the conclusions from point A. Point B shows an increased aluminium content in all three samples. Point C showed a decreased manganese and silicone content compared to the points closer to the weld section. The magnesium content was slightly higher for both LTT materials, but was less for the industry weld filler. In Point C, the magnesium and aluminium contents were higher for all three

cases. The silicone content was lower in both LTT materials but was higher in the industry weld filler. There was almost zero difference in magnesium content for both LTT materials, whereas the CIGWELD material had a significantly higher amount. The difference of silicone content between points D and C for CIGWELD is quite substantial, Point C has almost no difference to the base metal, whereas Point D has 0.4% difference. Table 8 shows the analysis of the crack composition when compared to the base material and point D of LTTB. This was done to gain an idea of the composition in the exact crack location rather than the approximate location of point D. This analysis was not done for all welds, as this crack face was unique to this test. The silicone content was significantly lower on the crack face when compared to the base material. It is likely that some of the points were not placed correctly, small adjustments to the positions may change the results significantly, the difference of 0.5 mm could be extreme. The three missing elements may have played a big role in percentages and the differences across the samples. Also, for consistency to the theoretical compositions, these three elements should be included in the SEM analysis.

Table 8. Crack chemical composition (LTTB).

Element	LTTB crack face					
	Compared to base			Compared to point D		
	Base (wt%)	ΔA	ΔB	D (wt%)	ΔA	ΔB
Mg	0.07	-0.01	0.20	0.28	-0.22	-0.01
Al	0.19	0.37	0.30	0.32	0.23	0.17
Si	6.99	-6.69	-6.29	1.03	-0.73	-0.34
Cl	0.04	0.04	-0.03	0.08	0.00	-0.07
K	0.02	0.09	-0.07	0.01	0.10	-0.06
Mn	0.79	0.05	0.02	0.82	0.02	-0.01
Fe	92.02	6.04	5.65	97.64	0.42	0.03

The hardness testing and SEM analysis showed some interesting patterns. The industry filler had the lowest hardness on the weld section, with both LTTA and LTTB having a similar value. Points 7, 8, 5 and 9 allow to analyse the magnitude of the hardness across the x-axis. Figure 9 shows the change in hardness as the points pass the HAZ. It is possible to conclude from these points that the hardness begins to decrease at point 8, reaching a minimum directly below the weld toe. Both LTT fillers reached a harder microstructure at point 3, in contrary to the industry filler, which has its lowest hardness at point 3. In general, points 4, 5, 8 and 9 were softer than the surrounding metal. Indeed, this is to be expected as these points are the most likely to correlate to the HAZ. Moreover, it is expected that points 4, 5 and

9 would undergo the largest change as these points are the closest to the weld material. Therefore experiencing the largest addition of heat and migration of elements.

The scanning electron microscope was used to better understand the chemical composition surrounding the weld toe, to aid in explaining the changes occurred throughout the weld process. The scanning electron microscope (SEM) examination showed a number of possible anomalies. Looking at the trends for point A, it can be seen that the manganese percentage was higher in all welds, which is expected because small amounts of manganese reduce sulphur brittleness, and is a hardening agent up to 1%, a desirable characteristic in welding applications. The Cigweld and LTTB welds showed a higher silicone content than the base metal while the LTTA had a lower silicone content. This is not surprising as the silicone weight percentage is lower in LTTA. The higher Silicone content is expected as it is an important element for altering weld fluidity and shrinkage, and it can increase the overall tensile strength. The higher manganese content is expected at point B as the weld material retains a higher manganese content for increased microstructure refinement [48]. LTTA and LTTB retained higher concentrations of silicone which is ideal for increased fluidity and decreased porosity [30]. The increased aluminium content is higher for all 3 materials. This is expected as aluminium can restrict grain growth which is advantageous in small quantities (less than 2%). Point C is the outermost chosen point, showing the chemical composition on the outer edge of the heat affected zone. The manganese content was lower for all cases but only by approximately 0.07%. This might mean that the manganese is slightly drawn into the weld during the cooling process. The silicone content was significantly lower in all cases, this shows that the HAZ lacks in silicone. In fact, this makes sense as silicon has a lower melting point and can easily migrate into weld during the cooling. Point D was the approximate location of the HAZ boundary. These results were expected to be the least consistent as it marks the border between two structures. This was not the case since point D showed 4 consistent trends.

The lower silicone content in both LTT materials is likely due to silicone has lower melting point, allowing it to move into the liquidised area during cooling. It is possible that due to the CIGWELD wire hardening at a higher temperature, it trapped a higher content of silicone in place. The silicone content difference between points D and C for CIGWELD is quite substantial: Point C has almost no difference to the base metal, whereas Point D has 0.4% increase. The significant silicone difference from point C to D means that there is a defined line where the silicone became more prominently, creating a defined transition zone, i.e. the HAZ boundary. When comparing the chemical compositions to the analysed crack face, it shows that silicone was significantly lower on the face at almost 0%, when compared to the base metal, at 6.9%. When comparing the crack composition to Point D of LTTB it shows that there is not any significant difference apart from the silicone content. This proves that point D was not directly on the crack location although it was extremely close. The 3 missing elements (C, Cr and Mo) may have played a major role in the percentages and the differences across the samples, also, for consistency compared to the theoretical compositions, these 3 elements should be included in this analysis. Although

LTTA has 0.85wt% nickel, in the SEM analysis it only showed small traces of nickel (Ni<0.005wt%). This means that the nickel disappeared during the welding process. The analysis of the Haz was conducted as secondary test, only performed to help explain the complicated phenomena. This analysis only gives a general idea of the effects around the weld and is partially reliant on the preparation of the samples. The samples were left rough which can greatly affect both the hardness testing and the SEM analysis. The SEM relies on properly prepared, clean and dry samples to relay the correct data, trace amounts of dirt or water can throw the weight percentage out. The chlorine content in many of the samples was reasonably high, this is likely due to the smoothing phase requiring the addition of tap water containing chlorine.

4. Conclusions

In this paper, both LTT materials were successful at improving the fatigue life. The lower martensite temperature decreased the residual stresses within the weld and therefore increased the life of the specimens. Bohler T160T slightly outperformed Lincoln 71E-H, with a longer fatigue life and lower residual stresses. The Bohler weld filler had the addition of 0.85wt% nickel with a carbon increase of 0.03wt% compared to the Lincoln 71E-H. The improved performance can be a result of the added nickel and increased carbon. The fatigue life testing showed that although the Lincoln weld filler had an overall lower life, its crack propagation outlasted the Bohler weld filler. This suggests that, although the Bohler filler has improved fatigue life it may have a more brittle structure leading to a shorter crack propagation. The weld analysis was a very successful investigation as the patterns found support in the previous literature and are reflected in the practical results. The hardness testing showed that the material surrounding the weld was significantly softer than the unaffected plate. The SEM analysis identified several chemical differences between the weld section, the HAZ, and the unaffected material. The migration of silicone and manganese was a major contributor to the residual stress and resulting fatigue life. Although the SEM analysis for chemical composition was helpful, an analysis on the microstructure may show even more interesting patterns. The computational results did not correlate with the overall life of the parts. This was explained by the excessive amount of unknowns when attempting to simulate the material alteration. The simulation did however relate to the point of failure, i.e. the toe of the weld is clearly the weak point, as this was identified in the simulation and every practical test alike.

References

[1] NEJAD R., 2020. “Numerical study on rolling contact fatigue in rail steel under the influence of periodic overload.” Engineering Failure Analysis, 115, 104624.

[2] MASOUDI NEJAD R., 2020. “The effects of periodic overloads on fatigue crack growth in a pearlitic Grade 900A steel used in railway applications.” Engineering Failure Analysis, 115, 104687.

[3] MASOUDI NEJAD R., ZHILIANG LIU, WENCHEN MA, FILIPPO BERTO, 2021. Fatigue reliability assessment of a pearlitic Grade 900A rail steel subjected to multiple cracks. Engineering Failure Analysis, 128:105625.

[4] SHARIATI M., MIRZAEI M., and MASOUDI R., 2018. "An applied method for fatigue life assessment of engineering components using rigid-insert crack closure model", Engineering Fracture Mechanics, 204, pp. 421-433.

[5] ZHILIANG LIU, WENCHEN MA, FILIPPO BERTO, 2021. Reliability analysis of fatigue crack growth for rail steel under variable amplitude service loading conditions and wear. International Journal of Fatigue, 152:106450.

[6] MASOUDI R., MOHAMMADREZA TOHIDI, AHMAD JALAYERIAN, AMIN SABER, MAHMOUD SHARIATI, 2020. "Experimental and numerical investigation of fatigue crack growth behavior and optimizing fatigue life of riveted joints in Al-alloy 2024 plates." Theoretical and Applied Fracture Mechanics, 108, 102669.

[7] MOAT, R., STONE, H., SHIRZADI, A., FRANCIS, J., KUNDU, S., MARK, A., BHADESHIA, H., KARLSSON, L. & WITHERS, P. 2011. Design of weld fillers for mitigation of residual stresses in ferritic and austenitic steel welds. Science and Technology of Welding and Joining, 16, 279-284.

[8] WITHERS, P., TURSKI, M., EDWARDS, L., BOUCHARD, P. & BUTTLE, D. 2008. Recent advances in residual stress measurement. International Journal of Pressure Vessels and Piping, 85, 118-127.

[9] WITHERS, P. J. & BHADESHIA, H. 2001. Residual stress. Part 1–measurement techniques. Materials science and Technology, 17, 355-365.

[10] ZHONG, Y., XIE, J., CHEN, Y., YIN, L., HE, P., LU, W. (2022). Microstructure and mechanical properties of micro laser welding NiTiNb/Ti6Al4V dissimilar alloys lap joints with nickel interlayer. Materials Letters, 306. doi: 10.1016/j.matlet.2021.130896

[11] WANG, H., XIE, J., CHEN, Y., LIU, W., & ZHONG, W. (2022). Effect of CoCrFeNiMn high entropy alloy interlayer on microstructure and mechanical properties of laser-welded NiTi/304SS joint. Journal of materials research and technology, 18, 1028-1037. doi: 10.1016/j.jmrt.2022.03.022

[12] LIANG, L., XU, M., CHEN, Y., ZHANG, T., TONG, W., LIU, H., LI, H. (2021). Effect of welding thermal treatment on the microstructure and mechanical properties of nickel-based superalloy fabricated by selective laser melting. Materials science & engineering. A, Structural materials: properties, microstructure and processing, 819, 141507. doi: 10.1016/j.msea.2021.141507

[13] WENCHEN MA. (2016). "Simulate initiation and formation of cracks and potholes," Master Report, Northeastern University, Boston, Massachusetts, USA, 93 p.

[14] LV, Z., GUO, J., & LV, H. (2022). Safety Poka Yoke in Zero-Defect Manufacturing Based on Digital Twins. IEEE transactions on industrial informatics, doi: 10.1109/TII.2021.3139897

[15] WENCHEN MA. (2021). "Behavior of Aged Reinforced Concrete Columns under High Sustained Concentric and Eccentric Loads," Doctoral Thesis, University of Nevada, Las Vegas, Nevada, USA, 198 p.

[16] ROSSINI, N., DASSISTI, M., BENYOUNIS, K. & OLABI, A.-G. 2012. Methods of measuring residual stresses in components. Materials & Design, 35, 572-588.

[17] LI, X., YANG, X., YI, D., LIU, B., ZHU, J., LI, J., WANG, L. (2021). Effects of NbC content on microstructural evolution and mechanical properties of laser cladded Fe50Mn30Co10Cr10-xNbC composite coatings. Intermetallics, 138. doi: 10.1016/j.intermet.2021.107309

[18] WEI, G., FAN, X., XIONG, Y., LV, C., LI, S., LIN, X. (2022). Highly disordered VO2 films: appearance of electronic glass transition and potential for device-level overheat protection. Applied physics express, 15(4). doi: 10.35848/1882-0786/ac605d

[19] BROWN, M. W. & MILLER, K. 1973. A theory for fatigue failure under multiaxial stress-strain conditions. Proceedings of the Institution of Mechanical engineers, 187, 745-755.

[20] TONG, J. 2001. Three stages of fatigue crack growth in GFRP composite laminates. J. Eng. Mater. Technol., 123, 139-143.

[21] ASGARIAN, B., P. MAZAHERI, and H. GHOLAMI. Comparison of fatigue life assessment of tubular joints using different editions of API RP-2A standards. Proceedings of the 10th National Conference on Structures and Steel, 2019, Tehran, Iran.

[22] ZHANG, C., W. MA, X. LIU, Y. TIAN, S. L. ORTON. (2019). "Effects of high temperature on residual punching strength of slab-column connections after cooling and enhanced post-punching load resistance," Engineering Structures, Vol 199, 109580.

[23] KIRKHOPE, K., BELL, R., CARON, L., BASU, R. & MA, K.-T. 1999. Weld detail fatigue life improvement techniques. Part 1. Marine structures, 12, 447-474.

[24] ÇAM, G., ÖZDEMIR, O. & KOÇAK, M. Progress in low transformation temperature (LTT) filler wires. Proceedings of the 63rd Annual Assembly & International Conference of the International Institute of Welding, 2010. 759-765.

[25] NIKNAM, B., F. ABOUTALEBI, W. MA, R. MASOUDI NEJAD. (2021). "Effect of variations internal pressure on cracking radiant coils distortion," Structures, Vol 34, pages 4986-4998.

[26] KROMM, A., KANNENGIESSER, T. & GIBMEIER, J. In situ observation of phase transformations during welding of low transformation temperature filler material. Materials Science Forum, 2010. Trans Tech Publ, 3769-3774.

[27] ZENITANI, S., HAYAKAWA, N., YAMAMOTO, J., HIRAOKA, K., MORIKAGE, Y., KUBO, T., YASUDA, K. & AMANO, K. 2007. Development of new low transformation temperature welding consumable to prevent cold cracking in high strength steel welds. Science and Technology of Welding and Joining, 12, 516-522.

[28] ECKERLID, J., NILSSON, T. & KARLSSON, L. 2003. Fatigue properties of longitudinal attachments welded using low transformation temperature filler. Science and Technology of Welding and Joining, 8, 353-359.

[29] DING, J., HUANG, H., MCCORMICK, P. & STREET, R. 1995. Magnetic properties of martensite-austenite mixtures in mechanically milled 304 stainless steel. Journal of magnetism and magnetic materials, 139, 109-114.

[30] EVANS, G. 1986. Effects of silicon on the microstructure and properties of C-Mn all-weld-metal deposits. Metal Construction, 18, 438R-444R.

[31] OLSON, D. 1985. Prediction of austenitic weld metal microstructure and properties. Welding journal, 64, 281s-295s.

[32] CHEN, F., JIN, Z., WANG, E. et al. Relationship model between surface strain of concrete and expansion force of reinforcement rust. Sci Rep 11, 4208 (2021). https://doi.org/10.1038/s41598-021-83376-w

[33] FAN-XIU, C., YI-CHEN, Z., XIN-YA, G., ZU-QUAN, J., EN-DONG, W., FEI-PENG, Z., XIAO-YUAN, H. (2020). Non-uniform Model of Relationship Between Surface Strain and Rust Expansion Force of Reinforced Concrete. Scientific Reports. doi: 10.1038/s41598-021-88146-2"

[34] HUA HUANG, M. A., HUANG, M., WEI ZHANG, M. A., POSPISIL, S., & WU, A. T. (2020). Experimental Investigation on Rehabilitation of Corroded RC Columns with BSP and HPFL under Combined Loadings. JOURNAL OF STRUCTURAL ENGINEERING, 146(8). doi: 10.1061/(ASCE)ST.1943-541X.0002725

[35] GUAN, H., HUANG, S., DING, J., TIAN, F., XU, Q., ZHAO, J. (2020). Chemical environment and magnetic moment effects on point defect formations in CoCrNi-based concentrated solid-solution alloys. Acta materialia, 187, 122-134. doi: 10.1016/j.actamat.2020.01.044

[36] MOUSAVI, A. A., ZHANG, C., MASRI, S. F., & GHOLIPOUR, G. (2021). Damage detection and characterization of a scaled model steel truss bridge using combined complete ensemble empirical mode decomposition with adaptive noise and multiple signal classification approach. Structural health monitoring, 84049285. doi: 10.1177/14759217211045901

[37] LIU, S., SAI, Q., WANG, S., & WILLIAMS, J. (2022). Effects of Laser Surface Texturing and Lubrication on the Vibrational and Tribological Performance of Sliding Contact. Lubricants, 10(10), 10. doi: 10.3390/lubricants10010010

[38] BROBERG, P. & RUNNEMALM, A. Detection of surface cracks in welds using active thermography. 18th World Conference on Nondestructive Testing, Durban, South Africa, 2012.

[39] XU, W., Y. LI, W. MA, K. LIANG, Y. YU. (2020). "Effects of spacing ratio on the FIV fatigue damage characteristics of a pair of tandem flexible cylinders," Applied Ocean Research, Vol 102, 102299.

[40] Xu, W., Q. ZHANG, W. MA, E. WANG. (2020). "Response of two unequal diameter flexible cylinders in a side-by-side arrangement: characteristics of FIV," China Ocean Engineering, Vol 34, pages 475-787.

[41] GREG WHEATLEY, A. O. 2002. Structural Integrity and Fracture. On fatigue life improvement using low transformation temperature weld material.

[42] KANNENGIESSER, T., RETHMEIER, M., PORTELLA, P. D., EWERT, U. & REDMER, B. 2011. Assessment of hot cracking behaviour in welds: Dedicated to Prof. Bernhard Wielage on the occasion of his 65th birthday. International journal of materials research, 102, 1001-1006.

[43] KARLSSON, L., MRÁZ, L., BHADESHIA, H., SHIRZADI, A. & ESAB AB, G. 2010. Comparison of alloying concepts for Low Transformation Temperature (LTT) welding consumables. Biuletyn Instytutu Spawalnictwa, 54, 33-9.

[44] HART, P. 1986. Resistance to hydrogen cracking in steel weld metals. Welding Journal, 65, 14s-22s.

[45] WU, S., WANG, D., ZHANG, Z., LI, C., LIU, X., MENG, X., FENG, Z. & DI, X. 2019. Mechanical properties of low-transformation-temperature weld metals after low-temperature postweld heat treatment. Science and Technology of Welding and Joining, 24, 112-120.

[46] CARVILL, J. 2012. Mechanical Engineers Data Handbook, Butterworth-Heinemann.

[47] POURKIA, N., MARASHI, P., LEYLABI, R., TABATABAEI, S. A. & TORSHIZI, H. The Effect of Weld Metal Manganese Content on the Microstructure, Mechanical Properties and Hot Crack Susceptibility of Helically Welded Linepipes. International Pipeline Conference, 2008. 101-106.

[48] KUMAR, V., MEHDI, H. & KUMAR, A. 2015. Effect of Silicon content on the Mechanical Properties of Aluminum Alloy. International Research Journal of Engineering and Technology, 2, 1326-1330.

Declaration of interests

☒ The authors declare that they have no known competing financial interests or personal relationships that could have appeared to influence the work reported in this paper.

☐The authors declare the following financial interests/personal relationships which may be considered as potential competing interests:

Highlights

- This paper aims at addressing the effect of the LTT filler on residual stress fields and fatigue lifetime
- The residual stress within each weld was quantified using the milling/strain gauge method
- The fatigue tests were conducted under uniaxial loading
- The results show that the crack propagation of all samples was similar in cycles although both LTT materials
- It was found that both LTT materials reduced the residual tensile stresses